

2 Aerosol optical depth over land: Comparing AERONET, AVHRR and 3 MODIS

4 A. Hauser, D. Oesch, and N. Foppa

5 Institute of Geography, University of Berne, Berne, Switzerland

6 Received 20 May 2005; revised 2 August 2005; accepted 17 August 2005; published XX Month 2005.

8 [1] Data from NOAA-16 AVHRR have been used to
9 retrieve the spatial distribution of aerosol optical depth for
10 central Europe. At eight AERONET sites, monthly mean
11 values based on daily AVHRR aerosol maps are calculated
12 and compared to monthly mean values from TERRA-
13 MODIS, AQUA-MODIS and AERONET. Additionally,
14 seasonal mean maps for 2002 are presented. To estimate the
15 performance of this algorithm, the winter and summer
16 season maps are compared to TERRA-MODIS seasonal
17 maps created from the daily global aerosol product. In
18 general, the AVHRR and MODIS aerosol maps show the
19 same features: Lower values with increasing altitude, higher
20 values in heavily industrialized areas and overall reasonable
21 mean values. AVHRR maps are spatially more
22 homogeneous than MODIS, which seem to contain an
23 imprint of the surface cover type. The maps clearly
24 demonstrate the potential of the retrieval method to
25 produce a climatology based on AVHRR aerosol optical
26 depth data over land. **Citation:** Hauser, A., D. Oesch, and
27 N. Foppa (2005), Aerosol optical depth over land: Comparing
28 AERONET, AVHRR and MODIS, *Geophys. Res. Lett.*, 32,
29 LXXXXX, doi:10.1029/2005GL023579.

31 1. Introduction

32 [2] The importance of aerosols for radiative and chemical
33 processes in the atmosphere is widely recognized. They can
34 scatter and/or absorb solar radiation leading to modifica-
35 tions of the radiation budget. Furthermore, the so-called
36 indirect effect of aerosols describes the cloud-aerosol inter-
37 actions, which can modify the chemical and physical
38 processes in the atmosphere. Their high spatial variability
39 and short lifetime make spaceborne sensors especially well
40 suited for their observation. Since the launch of the MODerate
41 resolution Imaging Spectroradiometer (MODIS) there is
42 detailed global aerosol information available, both over land
43 and oceans. The Advanced Very High Resolution Radiometer
44 (AVHRR) has also been used for the retrieval of aerosol
45 optical depth (AOD) but a global and continuous data set has
46 so far been restricted to oceans [Ignatov *et al.*, 1995, 2004].
47 Land surfaces are in general more difficult to characterize
48 since their surface reflectance might vary, e.g. due to a
49 vegetation cycle, and their bidirectional reflectance properties
50 are unknown. This has restricted most retrieval schemes to
51 dark dense vegetation surfaces [Kaufman and Sendra, 1988;
52 Soufflet *et al.*, 1997]. Hauser *et al.* [2005] presented a new
53 approach to retrieve AOD from NOAA AVHRR over land
54 regardless of the surface type, i.e. this method is applicable to

all land pixels which are not cloud or snow contaminated. 55
This paper focuses now on the spatial differences of AOD. 56
Monthly mean AOD from TERRA-MODIS, AQUA- 57
MODIS, NOAA-16 AVHRR and AERONET are shown as 58
time series for the year 2002. Additionally, we compare 59
seasonal mean maps of AOD over central Europe constructed 60
from the daily global MODIS aerosol product and daily 61
AVHRR AOD maps. 62

2. Data Set Summary 63

[3] AERONET (AErosol RObotic NETwork) is a feder- 64
ation of ground-based remote sensing instruments measur- 65
ing aerosol and its characteristics. The network imposes 66
standardization of instruments, calibration and processing 67
[Holben *et al.*, 1998]. The highest level product, the level 68
2.0 (cloud-screened [Smirnov *et al.*, 2000] and quality- 69
assured), was used in this study and the expected accuracy 70
of the AOD is about 0.01–0.02 [Eck *et al.*, 1999]. Measure- 71
ments are taken for an airmass of 7 or smaller at typically 15 72
minutes intervals. For 2002, level 2.0 data has been avail- 73
able for eight AERONET sites in our study region. In order 74
to compare AERONET and satellite retrieved AOD, the 75
AERONET optical thickness has to be determined for the 76
wavelength of 0.55 μm . Like the majority of comparable 77
studies, we continue to use a second order polynomial fit in 78
logarithm of wavelength [e.g., Ignatov *et al.*, 1995; Knapp 79
and Stowe, 2002]. Additionally, the best fit to measured 80
AERONET spectral AOD is the second order polynomial fit 81
[Eck *et al.*, 1999]. 82

[4] The AVHRR data set consists of daily full resolution 83
NOAA-16 afternoon passes from December 2001 through 84
end of December 2002. The region of interest is limited to 85
an area covering central Europe from 40.5°N to 50°N and 86
0°E to 17°E. The equator crossing at local time (EQX) of 87
NOAA-16 is at about 13:30 and typically one image per day 88
is recorded. The pre-processing includes calibration, precise 89
geocoding, orthorectification, cloud and cloud shadow 90
masking. For further details, see Hauser *et al.* [2005]. 91

[5] The daily global MODIS Collection 004 product 92
MOD04L2 (TERRA) and MYD04L2 (AQUA) from De- 93
cember 2001 through end of December 2002 have been 94
reprojected and resampled to the AVHRR grid. The aerosol 95
optical thickness products over land are accurate to within 96
their calculated uncertainties $\Delta\tau = \pm 0.05 \pm 0.20\tau$ [Chu *et al.* 97
et al., 2002; Remer *et al.*, 2005], except in situations with 98
possible cloud contamination, over surfaces with subpixel 99
surface water such as coastal areas and marshes, and over 100
surfaces with subpixel snow or ice cover. Due to some 101
overlap of the satellite passes in this region about two 102
images are taken during daytime per satellite, one taken at 103

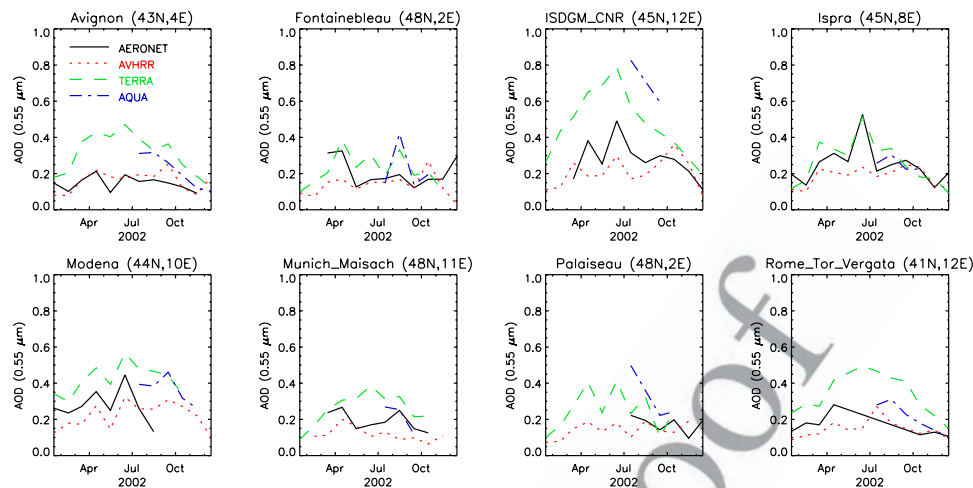


Figure 1. Time series of the aerosol optical depth from AERONET, NOAA-16 AVHRR, TERRA-MODIS and AQUA-MODIS.

104 about the nominal equator crossing time plus the previous
 105 or subsequent pass. TERRA is in a mid-morning orbit (EQX
 106 10:30) and AQUA in an afternoon orbit (EQX 13:30).
 107 Apparently, we must expect some differences between
 108 TERRA and NOAA-16 due to an EQX difference of about
 109 3 hours. *Smirnov et al.* [2002] investigated the diurnal cycle
 110 of AOD at different AERONET sites. For urban/industrial
 111 sites, there is generally an increase of AOD during the day.
 112 For Ispra they observed an increase of less than 10% and for
 113 Rome of 10–15%. However, from 10:30 to 13:30 the
 114 observed increase is significantly less. This finding is
 115 confirmed by *Ichoku et al.* [2005] by analyzing the morning
 116 (TERRA) and afternoon (AQUA) MODIS AOD. For West-
 117 ern Europe they found a weak average regional AQUA-
 118 TERRA difference of AOD at $0.55 \mu\text{m}$ of 0.007. The
 119 comparison of the MODIS TERRA to NOAA-16 AOD is
 120 therefore feasible.

121 3. Aerosol Retrieval From NOAA AVHRR Data

122 [6] The retrieval of AOD from NOAA AVHRR as
 123 described by *Hauser et al.* [2005] makes use of the high
 124 temporal resolution. The NOAA mid-morning and after-
 125 noon satellites generally provide daily coverage under
 126 sunlight conditions. To estimate the surface reflectance from
 127 AVHRR channel 1 ($0.63 \mu\text{m}$), a time series of observations
 128 covering the previous 44 days is used. Due to the orbital
 129 configuration of the NOAA satellites, all measurements are
 130 taken under various satellite zenith angles. It is further
 131 assumed that the surface target remains radiometrically
 132 stable and that some of the observations are made under
 133 background conditions. Plotting the surface reflectance as a
 134 function of the satellite zenith angle and applying a convex
 135 hull to the data, one can extract the surface reflectance for
 136 background conditions for the whole range of satellite
 137 zenith angles. The convex hull of a set of points on a single
 138 plane is defined as the smallest convex polygon that
 139 encloses these points. To identify the polygon points, a
 140 Delaunay triangulation algorithm has been used. When the
 141 surface and top of atmosphere reflectance are known, the
 142 SMAC [*Rahman and Dedieu*, 1994] radiative transfer code
 143 can be used to calculate the AOD using pre-defined aerosol

models. For Western Europe, a continental aerosol model 144
 [d'Almeida *et al.*, 1991] is most appropriate. To reduce 145
 noise, a MODIS-like procedure is applied: Inside a 25×25 146
 pixel region only pixels inside the 10–40 percentile are 147
 used to calculate a mean value. Additionally, the standard 148
 deviation of the AOD of these pixels is calculated. This 149
 parameter can be regarded as a quality measure. Low values 150
 indicate little AOD variations and high values point e.g. to 151
 cloud contamination. Based on the regional standard devi- 152
 ation of the AOD, a post-processing can be applied, which 153
 substantially increases the retrieval quality. 154

155 4. Results and Discussion

[7] Time series of AERONET, TERRA-MODIS, AQUA- 156
 MODIS and NOAA-16 AVHRR AOD are plotted in Figure 157
 1 at eight AERONET sites. For monthly means, at least 3 158
 records per month and pixel were needed for the calcula- 159
 tions. The correlation of AERONET and AVHRR time 160
 series are not discussed in detail since they are not inde- 161
 pendent data sets in this study. Only the development of the 162
 AVHRR retrieval scheme by *Hauser et al.* [2005] is based 163
 on coincident AERONET measurements, the found correla- 164
 tion is then assumed to be generally applicable. Even 165
 though, the AERONET monthly mean values contain much 166
 more data than used for the validation and includes also an 167
 additional AERONET site (ISDGM CNR), we focus on the 168
 comparison between AVHRR and MODIS data and try to 169
 explain apparent differences. In most cases, MODIS exhib- 170
 its the highest values but with good correlation to AERO- 171
 NET data. However, there is a substantial offset in AOD of 172
 about 0.2. *Abdou et al.* [2005] analyzed coincident TERRA 173
 Multiangle Imaging Spectroradiometer (MISR) and MODIS 174
 data at 62 AERONET stations during March, June and 175
 September 2002. Over land, MODIS is biased high compar- 176
 ed to MISR and AERONET, especially over deserts and 177
 sites with subpixel water contamination. Similar results are 178
 reported by *Ichoku et al.* [2005] by comparing AERONET 179
 data separately to TERRA and AQUA. Both are over- 180
 estimating the AERONET AOD but TERRA less than 181
 AQUA. *Remer et al.* [2005] also observed a positive bias 182
 at high optical thickness and suggest a calibration problem 183

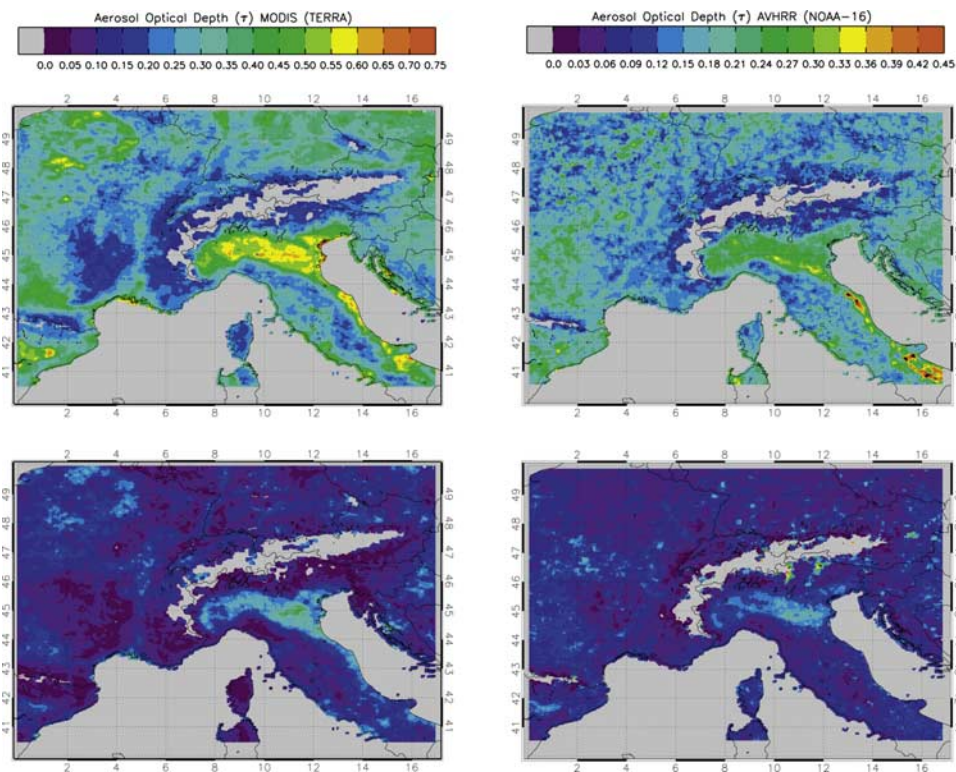


Figure 2. Aerosol optical depth distribution over central Europe for (top) summer and (bottom) winter 2002 for (left) TERRA-MODIS and (right) NOAA-16 AVHRR. Summer includes June, July and August 2002 data; winter includes December 2001, January and February 2002. Note the different color scale.

184 or, more likely, that the surface reflectance is improperly
 185 represented in a systematic way at certain locations and
 186 seasons.

187 [8] All time series show large month-to-month variations
 188 of the AOD and an annual cycle. The fact, that the data is
 189 acquired with different frequency and during different
 190 daytime, will be responsible for some differences between
 191 the data sets. Additionally, different cloud masking schemes
 192 are likely to bias the results. *Kinne et al.* [2003] report a
 193 MODIS tendency toward larger AOD averages with respect
 194 to AERONET. They link this effect to an AERONET
 195 preference for completely cloud-free conditions while
 196 MODIS can detect aerosols also near clouds. In the vicinity
 197 of clouds, AOD is frequently higher than in cloud-free
 198 areas.

199 [9] For seasonal means at least 9 records were required.
 200 The winter (December 2001, January 2002 and February
 201 2002) and summer (June, July and August 2002) aerosol
 202 distribution over central Europe are shown in Figure 2. The
 203 conclusions drawn from the winter and summer maps are
 204 also valid for the spring and fall maps, therefore only the
 205 more extreme winter and summer cases are displayed. To be
 206 able to discuss the regional distribution features of the two
 207 maps, a different scale has been applied since MODIS
 208 typically exceeds the AVHRR values by about 0.2. In
 209 general, the AVHRR and MODIS map show the same
 210 features: Lower values in mountainous regions like at the
 211 edge of the Alps (44°N–48°N/6°E–16°E) and the Pyrenees
 212 (42°N–43°N/0°E–3°E), higher values in heavily industri-
 213 alized areas and overall reasonable mean values. However,
 214 MODIS pronounces these features much more than

AVHRR. For example, the Massif Central (43°N–46°N/ 215
 2°E–5°E) is much more distinct in the MODIS map, 216
 compared to AVHRR. For winter and summer, high values 217
 are visible south of the Alps in northern Italy and on the 218
 east coast of Italy. This feature is present in both, the AVHRR 219
 and MODIS map. The most obvious differences between 220
 MODIS and AVHRR are found in northern France (47°N– 221
 50°N/0°E–5°E). In winter and summer, MODIS displays 222
 substantially higher values than AVHRR in this region. The 223
 shape of this feature matches well with predominantly 224
 agricultural land. Ground-based measurements from the 225
 AERONET stations in Fontainebleau and Palaiseau (Figure 226
 1) do not show any kind of different behavior than the other 227
 AERONET sites. The MODIS - AERONET offset is in the 228
 same order than for the other sites. The study by *Robles* 229
Gonzalez et al. [2000] using ATSR-2 for August 1997 does 230
 not show a similar feature as MODIS. Since it is only based 231
 on few data, this map can only be regarded as a further 232
 indication that MODIS might have problems in this region. 233
Holzer-Popp et al. [2002] present higher AOD in that 234
 region extracted from the synergetic use of GOME and 235
 ATSR-2 but the areal extent is much smaller and concen- 236
 trated around larger cities. Again, this study is based on few 237
 data from 1–3 September 1995. MODIS estimates the 238
 surface reflectance in the 0.66 μm channel by using a fixed 239
 relationship of half of the surface reflectance at 2.2 μm 240
 [Kaufman et al., 1997]. However, this relationship varies 241
 slightly depending on the surface cover. This leads to an 242
 imprint of the surface cover into the AOD data. We assume 243
 that the discussed feature is a surface reflectance related 244
 artifact, which is in line with the findings of *Remer et al.* 245

[2005]. The significant underestimation of AOD with respect to MODIS might be caused by differences in the single scattering albedo and/or surface reflectance. MODIS uses regionally pre-defined single scattering albedo and size distribution but allows for a varying mix of fine versus coarse mode fraction [Remer *et al.*, 2005]. AVHRR relies on pre-defined aerosol properties, even though the post-processing diminishes the effect of a too high single scattering albedo to a certain degree. Especially in highly industrialized areas, as northern Italy, high soot concentrations are expected and Mallet *et al.* [2005] showed that in polluted regions strong heterogeneities in aerosol single scattering albedo could occur even over short distances. These heterogeneities are not yet sufficiently considered in either the AVHRR or MODIS retrievals.

261 5. Conclusion

[10] For the first time, an AOD map over land from NOAA AVHRR has been shown. This map picks up the expected features and compares well with MODIS, even though differences are visible. The use of a fixed relationship between the MODIS 2.2 μm and 0.66 μm channels leads to an imprint of the surface cover into the AOD data. The AVHRR maps seem less sensitive to land cover types. The expected decrease of the AOD with increasing altitude is evident in both AVHRR and MODIS. Altogether, the AVHRR AOD map shows good results in the expected data range and correlates well to MODIS and AERONET data. The maps clearly demonstrate the potential of the applied retrieval method to produce AOD maps over land. This might lead to a climatology of AOD covering all NOAA AVHRR sensors.

[11] **Acknowledgments.** We would like to thank the AERONET PIs and their staff for establishing and maintaining the sites used in this study. Additionally, we thank MeteoSwiss, the National Center for Environmental Prediction and the EOS Data Gateway for supplying data and the Swiss Defense Procurement Agency for funding.

282 References

283 Abdou, W. A., D. J. Diner, J. V. Martonchick, C. J. Bruegge, R. A. Kahn, B. J.
284 Gaitley, and K. A. Crean (2005), Comparison of coincident Multiangle
285 Imaging Spectroradiometer and Moderate Resolution Imaging Spectroradiometer aerosol optical depths over land and ocean scenes containing
286 Aerosol Robotic Network sites, *J. Geophys. Res.*, *110*, D10S07,
287 doi:10.1029/2004JD004693.
288
289 Chu, D. A., Y. J. Kaufman, C. Ichoku, L. A. Remer, D. Tanré, and B. N.
290 Holben (2002), Validation of MODIS aerosol optical depth retrieval over
291 land, *Geophys. Res. Lett.*, *29*(12), 1617, doi:10.1029/2001GL013205.
292 d'Almeida, G., P. Koepke, and E. Shettle (1991), *Atmospheric Aerosols:
293 Global Climatology and Radiative Characteristics*, 561 pp., A. Deepak,
294 Hampton, Va.

Eck, T., B. Holben, J. Reid, O. Dubovik, A. Smirnov, N. O'Neill, I. Slutsker, 295
and S. Kinne (1999), Wavelength dependence of optical depth of biomass 296
burning, urban, and desert dust aerosols, *J. Geophys. Res.*, *104*, 31,333– 297
31,349. 298
Hauser, A., D. Oesch, N. Foppa, and S. Wunderle (2005), NOAA AVHRR 299
derived aerosol optical depth over land, *J. Geophys. Res.*, *110*, D08204, 300
doi:10.1029/2004JD005439. 301
Holben, B. N., et al. (1998), AERONET—A federated instrument network 302
and data archive for aerosol characterization, *Remote Sens. Environ.*, *66*, 303
1–16. 304
Holzer-Popp, T., M. Schroedter, and G. Gesell (2002), Retrieving aerosol 305
optical depth and type in the boundary layer over land and ocean from 306
simultaneous GOME spectrometer and ATSR-2 radiometer measure- 307
ments: 2. Case study application and validation, *J. Geophys. Res.*, 308
107(D24), 4770, doi:10.1029/2002JD002777. 309
Ichoku, C., L. A. Remer, and T. F. Eck (2005), Quantitative evaluation and 310
intercomparison of morning and afternoon Moderate Resolution Imaging 311
Spectroradiometer (MODIS) aerosol measurements from Terra and Aqua, 312
J. Geophys. Res., *110*, D10S03, doi:10.1029/2004JD004987. 313
Ignatov, A. M., L. L. Stowe, S. M. Sakerin, and G. K. Korotaev (1995), 314
Validation of the NOAA/NESDIS satellite aerosol product over the North 315
Atlantic in 1989, *J. Geophys. Res.*, *100*, 5123–5132. 316
Ignatov, A., J. Sapper, S. Cox, I. Laszlo, N. R. Nalli, and K. B. Kidwell 317
(2004), Operational aerosol observations (AEROBS) from AVHRR/3 on 318
board NOAA-KLM satellites, *J. Atmos. Oceanic Technol.*, *21*, 3–26. 319
Kaufman, Y. J., and C. Sendra (1988), Algorithm for automatic atmospheric 320
corrections to visible and near-ir satellite imagery, *Int. J. Remote Sens.*, *9*, 321
1357–1381. 322
Kaufman, Y., D. Tanré, L. A. Remer, E. F. Vermote, A. Chu, and B. N. 323
Holben (1997), Operational remote sensing of tropospheric aerosol over 324
land from EOS moderate resolution imaging spectroradiometer, *J. Geo-* 325
phys. Res., *102*, 17,051–17,067. 326
Kinne, S., et al. (2003), Monthly averages of aerosol properties: A global 327
comparison among models, satellite data, and AERONET ground data, 328
J. Geophys. Res., *108*(D20), 4634, doi:10.1029/2001JD001253. 329
Knapp, K. R., and L. L. Stowe (2002), Evaluating the potential for retrieving 330
aerosol optical depth over land from AVHRR pathfinder atmosphere 331
data, *J. Atmos. Sci.*, *59*, 279–293. 332
Mallet, M., V. Pont, and C. Liousse (2005), Modelling of strong hetero- 333
geneities in aerosol single scattering albedos over polluted region, *Geo-* 334
phys. Res. Lett., *32*, L09807, doi:10.1029/2005GL022680. 335
Rahman, H., and G. Dedieu (1994), SMAC: A simplified method for the 336
atmospheric correction of satellite measurements in the solar spectrum, 337
Int. J. Remote Sens., *15*, 123–143. 338
Remer, L. A., et al. (2005), The MODIS aerosol algorithm, products and 339
validation, *J. Atmos. Sci.*, *62*, 947–973. 340
Robles Gonzalez, C., J. Veeffkind, and G. de Leeuw (2000), Aerosol optical 341
depth over Europe in August 1997 derived from ATSR-2 data, *Geophys.* 342
Res. Lett., *27*, 955–958. 343
Smirnov, A., B. N. Holben, T. F. Eck, O. Dubovik, and I. Slutsker (2000), 344
Cloud screening and quality control algorithms for the AERONET data- 345
base, *Remote Sens. Environ.*, *73*, 337–349. 346
Smirnov, A., B. N. Holben, T. F. Eck, I. Slutsker, B. Chatenet, and R. T. 347
Pinker (2002), Diurnal variability of aerosol optical depth observed at 348
AERONET (Aerosol Robotic Network) sites, *Geophys. Res. Lett.*, 349
29(23), 2115, doi:10.1029/2002GL016305. 350
Soufflet, V., D. Tanré, A. Royer, and N. T. O'Neill (1997), Remote sensing 351
of aerosols over boreal forest and lake water from AVHRR data, *Remote* 352
Sens. Environ., *60*, 22–34. 353

N. Foppa, A. Hauser, and D. Oesch, Institute of Geography, University of 355
Berne, Hallerstr. 12, CH-3012 Berne, Switzerland. (adrian.hauser@web.de) 356